Radiocarbon dating of alpine ice cores with the dissolved organic carbon (DOC) fraction

Ling Fang[1,2,3], Theo M. Jenk[1,3,*], Thomas Singer[1,2,3], Shugui Hou[4,5], Margit Schwikowski[1,2,3]

*Corresponding author: Theo M. Jenk (theo.jenk@psi.ch)

[1]Laboratory for Environmental Chemistry, Paul Scherrer Institute, CH-5232 Villigen PSI, Switzerland

[2]Department of Chemistry and Biochemistry, University of Bern, CH-3012 Bern, Switzerland

[3]Oeschger Centre for Climate Change Research, University of Bern, CH-3012 Bern, Switzerland

[4]School of Geographic and Oceanographic Sciences, Nanjing University, Nanjing, 210023, China

[5]School of Oceanography, Shanghai Jiao Tong University, Shanghai 200240, China

Abstract

High-alpine glaciers are valuable archives of past climatic and environmental conditions. The interpretation of the preserved signal requires a precise chronology. Radiocarbon (^{14}C) dating of the water-insoluble organic carbon (WIOC) fraction has become an important dating tool to constrain the age of ice cores from mid-latitude and low-latitude glaciers. However, in some cases this method is restricted by the low WIOC concentration in the ice. In this work, we report first ^{14}C dating results using the dissolved organic carbon (DOC) fraction, which is present at concentrations of at least a factor of two higher than the WIOC fraction. We evaluated this new approach by comparison to the established WIO^{14}C dating based on parallel ice core sample sections from four different Eurasian glaciers covering an age range of several hundred to around 20'000 years. ^{14}C dating of the two fractions yielded comparable ages with WIO^{14}C revealing a slight, barely significant, systematic offset towards older ages comparable in magnitude with the analytical uncertainty. We attribute this offset to two effects of about equal size, but opposite in direction: (i) in-situ produced ^{14}C contributing to the DOC resulting in a bias towards younger ages and (ii) incompletely removed carbonates from particulate mineral dust (^{14}C depleted) contributing to the WIOC fraction with a bias towards older ages. The estimated amount of in-situ produced ^{14}C in the DOC fraction is smaller than the analytical uncertainty for most samples. Nevertheless, under extreme conditions, such as very high altitude and/or low snow accumulation rates, DO^{14}C dating results need to be interpreted cautiously. While during DOC extraction the removal of inorganic carbon is monitored for completeness, the removal for WIOC samples was so far only assumed to be quantitative, at least for ice samples containing average levels of mineral dust. Here we estimated an average removal efficiency of 98±2 %, resulting in a small offset in the order of the current analytical uncertainty. Future optimization of the removal procedure has the potential to improve the accuracy and precision of WIO^{14}C dating. With this study we demonstrate, that using the DOC fraction for ^{14}C dating is not only a valuable alternative to the use of WIOC, but also benefits from a reduced required ice mass of typically ~250 g to achieve comparable precision of around ±200 years. This approach thus has the potential of pushing radiocarbon dating of ice forward even to remote regions where the carbon content in the ice is particularly low.

1 Introduction

For a meaningful interpretation of the recorded paleoclimate signals in ice cores from glacier archives, an accurate chronology is essential. Annual layer counting, supported and tied to independent time markers such as the 1963 nuclear fallout horizon evident by a peak maximum in tritium or other radioisotopes, or distinct signals from known volcanic eruptions in the past is the fundamental and most accurate technique used for ice core dating. However, for ice cores from high-alpine glaciers this approach is limited to a few centuries only, because of the exceptional strong thinning of annual layers in the vicinity of the bedrock. Most of the current analytical techniques do not allow high enough sampling resolution for resolving seasonal fluctuations or detecting distinct single events in this depth range. Ice flow models, which are widely used to retrieve full depth age scales (e.g. Nye, 1963; Bolzan, 1985; Thompson et al., 2006), also fail in the deepest part of high-alpine glaciers due to the assumption of steady state conditions and the complexity of glacial flow and bedrock geometry limiting realistic modeling of strain rates. Even with 3D models, which require extensive geometrical data, it is highly challenging to simulate a reasonable bottom age (e.g. Licciulli et al., 2020). This emphasizes the need for an absolute dating tool applicable to the oldest, bottom parts of cores from these sites.

Radioactive isotopes contained in the ice offer the opportunity to obtain absolute ages of an ice sample. For millennial scale ice cores, ^{14}C dating is the technique of choice. With a half-life of 5370 years, dating in the age range from ~250 years to up to ten half-life times is theoretically possible, covering the time range accessible by alpine glaciers in the vast majority of cases (Uglietti et al., 2016). The ^{14}C dating approach using water insoluble organic carbon (WIOC) from glacier ice has become a well-established technique for ice core dating and its accuracy was recently validated (Uglietti et al., 2016). Ice samples from mid- and low-latitude glaciers can now be dated with a reasonable uncertainty of 10-20%. Ice sample masses of 200-800 g are usually selected to aim for >10 µg carbon for ^{14}C analysis with accelerator mass spectrometry (AMS), whereby the respective mass depends on sample age and organic carbon concentrations (Jenk et al., 2007; Jenk et al., 2009; Sigl et al., 2009; Uglietti et al., 2016; Hoffmann et al., 2018). Accordingly, the low WIOC concentration in some glaciers and in Polar Regions and the related large demands of ice mass puts a limit to this application. Concentrations of dissolved organic carbon (DOC) in glacier ice are a factor of 2-8 higher compared to typical WIOC concentrations (Legrand et al., 2007; Legrand et al., 2013; May et

al., 2013, Fang et al., in prep.). Using the DOC fraction for ^{14}C dating could therefore reduce the required amount of ice or, for sample sizes similar to what would be needed for ^{14}C dating by WIOC, improve the achievable analytical (dating) precision which strongly depends on the absolute carbon mass even for state-of-the-art micro-radiocarbon dating. The underlying hypothesis of applying the DOC fraction for ^{14}C dating is the same as for the WIO^{14}C dating approach (Jenk et al., 2006; Jenk et al., 2007; Jenk et al., 2009). DOC in ice is composed of atmospheric water soluble organic carbon (WSOC) contained in carbonaceous aerosol particles and organic gases taken up during precipitation (Legrand et al., 2013). WSOC is formed in the atmosphere by oxidation of gases emitted from the biosphere or from anthropogenic sources (Legrand et al., 2013; Fang et al. in prep.) and subsequent condensation of the less volatile products. Carbonaceous aerosols transported in the atmosphere can be deposited on a glacier by wet and dry deposition. Before the industrial revolution, these organic carbon species, then entirely of non-fossil origin, contain the contemporary atmospheric ^{14}C signal of the time when the snow deposited on the glacier (Jenk et al., 2006). For both WIOC and WSOC, carbon from biomass burning and oceanic organic matter can potentially introduce a reservoir effect (sources of aged carbon). The mixed age of trees in Swiss forests today is estimated to be slightly less than 40 years (Mohn et al., 2008). Back in time, prior to extensive human forest management, the mixed age of trees in Europe was likely older and the mean age of old-growth forest wood ranged from around 70 to 300 years depending on the region, i.e. the tree species present (Gavin, 2001, Zhang et al., 2017). Prior to the use of fossil fuels about 50% of WIOC is estimated to originate from biomass burning (Minguillon et al., 2011). For biogenic DOC, May et al. (2013) estimated a turnover-time of around 3 to 5 years, corresponding to a 20% contribution from biomass burning. With a mean age of burned material (aged wood plus grass and bushes) of 150±100 years, this results in a potential in-built age from biomass burning for WIOC and DOC of 75±50 and 30±20 years, respectively. Such an in-built age is negligible considering the analytical uncertainty, which is similarly the case for a bias from oceanic sources, since concentrations of marine organic tracers are more than one order of magnitude lower than terrestrial tracers for the vast majority of glacier sites. This conclusion is supported by the fact that Uglietti et al. (2016) did not identify such a bias, when comparing WIO^{14}C ages with ages derived by independent methods.

For analyzing DO^{14}C in ice cores, one of the major limitations is the relatively low extraction efficiency ranging from 64 % (Steier et al., 2013) to 96 % (May et al., 2013; Fang et al., 2019) and the high risk of sample contamination (Legrand et al., 2013) potentially

introduced during drilling, storage, and sample processing. A first attempt to use DOC for ^{14}C dating of ice samples was conducted by May (2009) using a set-up for a combined analysis of both, the DOC and WIOC fraction with subsequent radiocarbon micro-analysis. However, these first results suggested a potential in-situ production of ^{14}C in the DOC fraction based on the obtained super modern $F^{14}C$ values (i.e. $F^{14}C$ values higher than ever observed in the recent or past ambient atmosphere). Building on these initial findings, May (2009) questioned the applicability of the DOC fraction for radiocarbon dating. Although the in-situ ^{14}C production of ^{14}CO and $^{14}CO_2$ in air bubbles contained in polar ice has been studied thoroughly and is well understood (Van de Wal et al., 1994; Lal et al., 1997; Smith et al., 2000), possible mechanisms of ^{14}C in-situ production followed by formation of organic compounds are not and only few studies exist to date (Woon, 2002; Hoffmann, 2016). To further explore the potential of $DO^{14}C$ for dating ice, a DOC extraction setup for radiocarbon analyses was designed and built at the Paul Scherrer Institut (PSI). In order to minimize potential contamination, the entire system is protected from ambient air by inert gas (helium) flow or vacuum. To maximize the oxidation efficiency, the PSI DOC methodology applies an ultraviolet (UV) photochemical oxidation step supported by addition of Fenton's reagent. The setup has been characterized by a high extraction efficiency of 96% and a low overall process blank being superior in the resulting blank to sample ratio compared to other systems (Fang et al., 2019). The system can handle samples with volumes of up to ~350 mL. With this volume, samples with DOC concentrations as low as 25-30 µg/kg can be analyzed, yielding the minimal carbon mass required for reliable ^{14}C analysis (~10 µg C). Pooling samples from several subsequent extractions would be feasible, allowing dating of samples with lower DOC concentration. In this study, we evaluate ^{14}C dating with the DOC fraction by comparing to results from the well- established and validated $WIO^{14}C$ dating method. This is not only analytically highly challenging, but also because of the very limited availability of the precious sampling material needed in a rather large quantity (total for both fractions > 500 g), ideally covering a wide range of ages from a few hundred to several thousands of years. Here, we succeeded to analyze such parallel samples from four different Eurasian glaciers.

2 Sample preparation and ^{14}C analysis

To validate the DOC ^{14}C dating technique, a total of 17 ice sections from the deep parts of ice cores from the four glaciers Colle Gnifetti, Belukha, Chongce (Core 1), and Shu Le Nan Shan

(SLNS) were selected (Figure 1). They were sampled in parallel to directly compare DOC and WIOC concentrations and ^{14}C dating results. The high-alpine glacier Colle Gnifetti is located in the Monte Rosa massif of the Swiss Alps, close to the Italian border. A 76 m long core was retrieved from the glacier saddle in September 2015 at an altitude of 4450 m asl. (45°55'45.7''N, 7°52'30.5''E; Sigl et al., 2018), only 16 m away from the location of a previously dated core obtained in 2003 (Jenk et al., 2009). The low annual net accumulation rate at this site (~0.45 m w.e. yr^{-1}) provides access to old ice covering the Holocene (Jenk et al., 2009). Four samples were selected from the bottom 4 m closest to bedrock (72-76 m depth). The Belukha core was drilled in May/June 2018 from the saddle between the two summits of Belukha (49°48'27.7"N, 86°34'46.5"E, 4055 m asl.), the highest mountain in the Altai mountain range. The bedrock was reached and the total length of the core is 160 m. Three samples were analyzed from the deepest part (158-160 m). Seven, and three samples were analyzed from the deep parts of SLNS and Chongce, respectively. The SLNS ice core was retrieved in May 2010 from the south slope of the Shu Le Nan Shan Mountain (38°42'19.35"N, 97°15'59.70"E, 5337 m asl.). The bedrock was reached and the total length of the ice core is 81.05 m (Hou et al., submitted). The Chongce ice cap is located in the western Kunlun Mountains on the northwestern Tibetan Plateau, covering an area of 163.06 km^2 with a volume of 38.16 km^3 (Hou et al., 2018). The ice analyzed in this study was sampled from Chongce Core 1, one of three ice cores drilled in October 2012 (35°14'5.77"N, 81°7'15.34"E, 6010 m asl.). Two of those cores reached bedrock with lengths of 133.8 m (Core 1) and 135.8 m (Core 2). In 2013, two more ice cores were recovered from a higher altitude of 6100 m asl., reaching bedrock with lengths of 216.6 m (Core 4) and 208.6 m (Core 5) (Hou et al., 2018). The annual net accumulation rate is about 0.14 m w.e. yr^{-1} for Core 3, located less than 2 km away from Core 1. A summary of the metadata for the study sites and ice cores can be found in the supplement (Table S1) and details about sampling depths and sample sizes in Table 1. No results from any of the cores analyzed in this study have been published previously.

All sampled ice sections were decontaminated in a cold room (-20ºC) by cutting off the surface layer (~3 mm) and each section split into two parallel samples to perform both WIOC and DOC ^{14}C analysis. Samples for WIO^{14}C-dating were prepared following the protocol described in Uglietti et al. (2016) with a brief summary provided in the following. In order to remove potential contamination in the outer layer of the ice core, pre-cut samples from the inner part of the core were additionally rinsed with ultra-pure water (Sartorius, 18.2 MΩ×cm, TOC < 5ppb), resulting in samples masses ranging from ~300 to 600 g (Table 1). To dissolve

carbonate potentially present in the ice, melted samples were acidified with HCl to pH < 2, before being sonicated for 5 min. Subsequently, the contained particles were filtered onto pre-baked (heated at 800 °C for 5 h) quartz fiber filters (Pallflex Tissueqtz-2500QAT-UP). In a second carbonate removal step, the filters were acidified 3 times with a total amount of 50 μL 0.2M HCl, left for 1 h, rinsed with 5 mL ultra-pure water and finally left again for drying. These initial steps were performed in a laminar flow box to ensure clean conditions. At the Laboratory for the Analysis of Radiocarbon with AMS (LARA) of the University of Bern the particle samples were then combusted in a thermo-optical OC/EC analyzer (Model4L, Sunset Laboratory Inc, USA) equipped with a non-dispersive infrared (NDIR) cell to quantify the CO_2 produced, using the well-established Swiss 4S protocol for OC/EC separation (Zhang et al., 2012). Being coupled to a 200 kV compact accelerator mass spectrometer (AMS, MIni CArbon DAting System MICADAS) equipped with a gas ion source via a Gas Interface System (GIS, Ruff et al., 2007; Synal et al., 2007, Szidat et al., 2014), the LARA Sunset-GIS-AMS system (Agrios et al., 2015; Agrios et al., 2017) allowed for final, direct online ^{14}C measurements of the CO_2 produced from the WIOC fraction.

For $DO^{14}C$ analysis, sample preparation follows the procedure described in Fang et al. (2019). After transfer of pre-cut samples to the laboratory and before being melted, samples were further decontaminated in the pre-cleaned melting vessel of the extraction setup by rinsing with ultrapure water (sample mass loss of about 20-30 %), all performed under helium atmosphere. Simultaneously, a pre-cleaning step was applied to remove potential contamination in the system. For this, 50 mL ultra-pure water was injected into the reactor and acidified with 1 mL of 85% H_3PO_4. To enhance the oxidation efficiency, 2 mL of 100 ppm $FeSO_4$ and 1 mL of 50 mM H_2O_2 (Fenton's reagent) was also injected into the base water before turning on the UV lights for ~20 min, thereby monitoring the process via the online NDIR CO_2 analyzer. After the ice melted, the meltwater was filtrated under helium atmosphere, using a pre-baked in-line quartz fiber filter. The sample volume was determined by measuring the reactor fill level. The filtrate was acidified by mixing with the pre-treated base water. After degassing of CO_2 from inorganic carbon was completed as monitored by the CO_2- detector, 1 mL of 50 mM H_2O_2 was injected into the reactor right before the irradiation started. During UV oxidation, water vapor was removed by cryogenic trapping at -60 °C and produced CO_2 was trapped in liquid nitrogen. All steps were carried out under a constant flow of helium. The sample CO_2 was further cleaned from residual water vapor and quantified manometrically before being sealed into a glass vial for offline ^{14}C analyses. The CO_2 gas from DOC in the

glass vial was directly injected into the MICADAS using a cracking system for glass vials under vacuum, allowing to then carry the CO_2 gas in a helium flow to the AMS ion source (Wacker et al., 2013). Procedural blanks were determined and continuously monitored by processing and analyzing frozen ultra-pure water (Sartorius, 18.2 MΩ cm, TOC< 5ppb) similar to natural ice samples. They were prepared every time when cutting ice and then processed/analyzed along with the samples at least twice a week. Procedural blanks are 1.3±0.6 µg C with an $F^{14}C$ of 0.69±0.15 (n=76) and 1.9±1.6 µg C with an $F^{14}C$ value of 0.68±0.13 (n=30) for WIOC and DOC, respectively.

All ^{14}C results are expressed as fraction modern ($F^{14}C$), which is the $^{14}C/^{12}C$ ratio of the sample divided by the same ratio of the modern standard referenced to the year 1950 (NIST, SRM 4990C, oxalic acid II), both being normalized to -25‰ in $\delta^{13}C$ to account for isotopic fractionation. All AMS $F^{14}C$ values presented here are finally corrected for the system and method characteristic contributions as reported previously (e.g. Uglietti et al., 2016 and Fang et al., 2019). For WIOC analysis using the Sunset-GIS-AMS system this includes a correction for the system background, i.e. constant contamination (0.91±0.18 µgC with $F^{14}C$ of 0.72±0.11). For the cracking system applied for DOC samples the constant contamination is 0.06±0.18 µgC with $F^{14}C$ of 0.50 ±0.11). Further corrections applied account for the AMS cross contamination (0.2% of the previous sample), and procedural blanks (see above). All uncertainties were propagated throughout data processing until final ^{14}C calibration. These corrections, have a larger effect on low carbon mass samples (higher noise-to-sample ratio), resulting in a larger dating uncertainty. Therefore, we only discuss samples with a carbon mass larger than 10 µg as recommended in Uglietti et al. (2016). Radiocarbon ages are calculated following the law of radioactive decay using 5570 years as the half-life of radiocarbon, thus age equals -8033 * ln ($F^{14}C$) with -8033 years being Libby's mean lifetime of radiocarbon. Radiocarbon ages are given in years before present (BP) with the year of reference being 1950 (Stuiver and Polach, 1977). To obtain calibrated ^{14}C ages, the online program OxCal v4.3.2 with the IntCal13 radiocarbon calibration curve was used (Reimer et al., 2013; Ramsey, 2017). Calibrated ages, also given in years before present, are indicated with (cal BP) and denote the 1σ range unless stated otherwise.

3 Results

3.1 DOC and WIOC concentrations

DOC concentrations are generally higher compared to the corresponding WIOC concentrations (Figure 2). For all samples from the four glaciers, the DOC/WIOC concentration ratio ranges from 1.2 to 4.0 with an average of 1.9 ± 0.6 (Table 2). This is at the lower end of previously reported average DOC/WIOC ratios of 2-8 (Legrand et al., 2007; Legrand et al., 2013, Fang et al., in prep.). This is likely explained by temporal variability because most samples in this study are several thousand years old, whereas the literature data only covers the last few centuries, including values from the industrial period in which additional anthropogenic sources exist (e.g. fossil DOC precursors). It is interesting to note that the average DOC/WIOC ratio at Belukha (2.5) is higher compared to the other sites (Colle Gnifetti, SLNS and Chongce is 1.8, 1.7 and 1.6, respectively). Because the Belukha glacier is surround by extensive Siberian Forests, the higher ratio may be explained by particularly high emissions of biogenic volatile organic compounds. This is corroborated by the observation that DOC concentrations are highest at this site (241 ± 82 µg/kg) (Figure 2). Absolute concentrations of DOC and WIOC are slightly lower at Colle Gnifetti (112 ± 12 µg/kg and 63 ± 13 µg/kg, respectively) compared to the other three glaciers (Table 1 and 2). Mean DOC and WIOC concentrations in the ice from the Tibetan Plateau are 211±28 µg/kg and 123±19 µg/kg for SLNS and 156±40 µg/kg and 99±37 µg/kg for Chongce, respectively. These values are higher compared to the pre-industrial (PI) average values found in European Alpine glaciers, not only compared to the few samples from Colle Gnifetti of this study, but also to previously reported values from the Fiescherhorn glacier with PI-DOC of ~95 µg/kg (Fang et al., in prep.) and PI-WIOC of ~30 µg/kg (Jenk et al., 2006), respectively; and from Colle Gnifetti with PI-WIOC of ~30 µg/kg (Legrand et al., 2007; Jenk et al., 2006).

3.2 Radiocarbon results

For all four sites, $F^{14}C$ of both fractions (WIOC and DOC) decreases with depth, indicating the expected increase in age (Figure 2, Table 1 and 2). For three of the sites (Colle Gnifetti, Belukha and SLNS), the corresponding DOC and WIOC fractions yielded comparable $F^{14}C$ values with no statistical evidence for a significant difference (Mann-Whitney U-test, U=79.5, n=14, p=0.41>0.05). They scatter along the 1:1 ratio line, are significantly correlated (Pearson correlation coefficient r=0.986, $p < .01$, n=14) and both intercept (0.025 ± 0.034) and slope

(1.034 ± 0.050) are not significantly different from 0 and 1, respectively (Figure 3). Nevertheless, a slight systematic offset towards lower $F^{14}C$ values for WIOC compared to DOC seems evident if looking at Figures 2 and 3. This is particularly obvious for the samples from Chongce, characterized by high mineral dust load and from a site of very high elevation with low net accumulation. For these samples, the $F^{14}C$ DOC-WIOC offset is significant (discussion in Sect. 4.2 and 4.3).

For all sites, the calibrated ^{14}C ages from both fractions show an increase in age with depth (Table 3). The ages range from ~0.2 to 20.3 kyr cal BP for DOC and ~0.8 to 22.4 kyr cal BP for WIOC, respectively. In both fractions, the oldest age was derived for the sample from the deepest part of the Belukha ice core. Samples from Colle Gnifetti generally showed younger ages (< 2 kyr cal BP). The two ice cores from the Tibetan Plateau (SLNS and Chongce) cover a similar age span from ~0.2±0.1 to 5.5±0.3 kyr cal BP in the DOC fraction. $WIO^{14}C$ resulted in a similar age range for the samples from SLNS (0.8±0.4 to 6.6±0.8 kyr cal BP), but was considerably older for Chongce (3.1±0.7 to 11.0±1.7 kyr cal BP, discussion in Sect. 4.2 and 4.3).

4 Discussion

4.1 Radiocarbon dating with the DOC fraction

In Table 3, we present the first radiocarbon dating results of ice using the DOC fraction. The DOC calibrated ^{14}C age of ice increases with depth for all four sites, as expected for undisturbed glacier archives from the accumulation zone. For samples from three out of the four sites, our results (Sect. 3) indicate no significant difference in $F^{14}C$ between DOC and WIOC, with the latter fraction being validated for allowing accurate dating of the surrounding ice (Uglietti et al., 2016). With the new $DO^{14}C$ dating method an average dating uncertainty of around ±200 years was achieved for samples with an absolute carbon mass of 20-60 μg and ice younger than ~6 kyrs (Table 2 and 3). The analytical uncertainty mainly arises from correction for the procedure blank introduced during sample treatment prior to AMS analysis (see Sect. 2 for details about other corrections), contributing with 20 to 70 % to the final overall dating uncertainty. The contribution thereby depends on carbon mass (larger for small samples) and sample age (larger the bigger the difference between sample and blank $F^{14}C$). How the overall analytical uncertainty of $F^{14}C$ decreases with higher carbon mass is shown in Figure S1. For

DOC concentrations observed in this study, an initial ice mass of about 250 g was required, with about 20-30 % of the ice being removed during the decontamination processes inside the DOC set-up, yielding ~200 g of ice available for final analysis. Expected based on previously reported DOC/WIOC concentration ratios (Sect. 3.1), the results here confirmed that with this new technique, the required ice mass can be reduced by more than a factor of two compared to the mass needed for ^{14}C dating using the WIOC fraction. Consequently, using the DOC instead of the WIOC fraction for ^{14}C dating, a higher dating precision can be achieved for ice samples of similar mass. An additional benefit is that the DOC extraction procedure allows monitoring the removal of inorganic carbon for completeness (see Sect. 2), which is important to avoid a potential age bias (see Sect. 4.3).

4.2 Potential contribution of ^{14}C in-situ production to DO^{14}C

Previous studies suggested that ^{14}C of the DOC fraction may be influenced by in-situ production of ^{14}C in the ice matrix (May 2009; Hoffman 2016). Induced by cosmic radiation, the production of ^{14}C atoms within the ice matrix, i.e. by spallation of oxygen within the water molecule, is a well-known process (Lal et al., 1987; Van de Wal et al., 1994). Earlier studies indicated that in-situ produced ^{14}C atoms mostly form CO, CO_2 and CH_4 (Petrenko et al., 2013), but also can form methanol and formic acid (Yankwich et al., 1946, Woon, 2002). The mechanism of incorporation of in-situ produced ^{14}C incorporation into organic molecules is not well understood (Woon, 2002; Hoffman, 2016). Hoffmann (2016) performed neutron irradiation experiments on Alpine glacier ice, showing that about 11-25 % of the initially produced ^{14}C atoms entered into the DOC fraction. The resulting effect on F^{14}C of DOC consequently depends on (i) the number of ^{14}C atoms produced in the ice (^{14}C in-situ production), (ii) the fraction of these atoms incorporated into DOC, and because F^{14}C is based on a $^{14}C/^{12}C$ ratio, (iii) the DOC concentration in the ice (the higher the smaller the resulting shift in F^{14}C-DOC).

The natural neutron flux, relevant for the ^{14}C production rate, strongly depends on altitude and latitude with a generally uniform energy distribution of the incoming neutrons (Gordon et al., 2004). The ^{14}C in-situ production in natural ice further depends on the depth in the glacier and the snow accumulation rate of the site (Lal et al., 1987), determining the totally received neutron radiation. Following Lal et al. (1987), the number of in-situ produced ^{14}C

atoms in each of our ice samples was estimated, assuming an average incorporation into DOC of 18±7 % (Hoffmann, 2016) (Table 4, equations and input parameters in the Supplementary Material). The average $F^{14}C$-DOC shift for all samples is 0.044±0.033. We find a good correlation between the measured $F^{14}C$ DOC-WIOC offset and the ^{14}C in-situ caused $F^{14}C$-DOC shift which explains about 50 % of the offset (Pearson r=0.82, Figure 4) and after correcting for it improves the overall agreement between $F^{14}C$ of DOC and WIOC (Figure 5). The shift is largest for the Chongce samples (0.109±0.048) as a result of the high production rate at 6 km altitude in combination with the low annual net accumulation rate at this site (0.14 m w.e. yr^{-1}). The calculated shift for samples from the SLNS core, from similar latitude but from a site lower in altitude (5 km) and experiencing higher net accumulation (0.21 m w.e. yr^{-1}), is significant lower with 0.038±0.016. The samples from Belukha and Colle Gnifetti are least affected (0.013±0.006 and 0.033±0.013, respectively).

We find that while the effect of in-situ ^{14}C production causes only a negligible shift in $F^{14}C$-DOC for most samples (masked by the analytical uncertainty), it can become significant for ice samples from sites of exceptional high altitude and experiencing low annual net accumulation rates in addition, such as the Chongce ice cap (6010 m asl., 0.14 m w.e. yr^{-1}; Figure 4). Note that for any site, the size of this effect gets reduced the higher the DOC concentration of the sample.

4.3 Potential contribution of carbonates to ^{14}C of WIOC

Under the basic assumption that the initially emitted fractions of DOC and WIOC are of similar age, an additional contribution from ^{14}C-depleted carbonate (low $F^{14}C$) to the WIOC would cause an $F^{14}C$ offset between the two fractions. Previously published WIOC ^{14}C ages from the upper parts of the Chongce Core 2 and Core 4, less than 2 and ~6 km away from Core 1, did show large scatter with no clear increase in age with depth for samples younger than 2 kyrs. It was speculated that this was at least partly caused by the visible, exceptionally high loading of mineral dust on the WIOC filters (Hou et al., 2018). Such high mineral dust loading was also observed during filtration of the Chongce Core 1 samples presented here. High mineral dust content in the ice can influence ^{14}C dating with WIOC in two ways, by affecting filtration through clogging of the filter and by potentially contributing with ^{14}C-depleted carbon from carbonate, as has been discussed in most previous studies. They all concluded, that although

for dust levels typically observed in ice cores from high elevation glaciers no significant bias is detectable for ^{14}C of WIOC, it is of concern for the elemental carbon (EC) fraction combusted at higher temperatures during OC/EC separation. EC – as well as total carbon (TC, the sum of OC and EC) – is thus not recommended to be used for radiocarbon dating (Jenk et al., 2006; Jenk et al., 2007; Jenk et al., 2009; Sigl et al., 2009; Uglietti et al., 2016). In any case, the carbonate removal efficiency during WIOC sample preparation was never quantified.

Here, the hypothesis that incomplete removal of carbonate may have caused the $F^{14}C$ DOC-WIOC offset remaining after accounting for $DO^{14}C$ in-situ production (Sect. 4.2) was tested. Applying an isotopic mass balance based model to our dataset, the carbonate removal efficiency in $WIO^{14}C$ samples was estimated. The Ca^{2+} concentration in the ice samples was thereby used as a tracer for calcium carbonate (see Supplement for details).

We find a carbonate removal procedure incomplete by around 2 % (i.e. an average removal efficiency of 98±2 %) to be sufficient for explaining the remaining part of the observed $F^{14}C$ DOC-WIOC offset Figure 5). In terms of residual carbonate carbon mass on the filter, this equals to < 2 μgC on average (Table S2). On the one hand, this is in agreement with the findings of previous studies, indicating that the potential carbonate related bias for ^{14}C dating using WIOC is hardly detectable for ice samples with normal dust loading (effect masked by the analytical uncertainty, see Figure S2). For example, Uglietti et al. (2016) did not detect such an effect when successfully validating $WIO^{14}C$ dating results with ages from independent methods. On the other hand, it demonstrates that a slightly below average removal efficiency for ice samples containing visibly high loading of mineral dust can already cause a notable offset (93-97 % for Chongce). The likely bigger particle size in such samples will affect their solubility, i.e. increase the dissolution time required in the acid treatment step. In the current procedure, this time is not adjusted accordingly (Sect. 2). Based on these results, we consider a small offset from incomplete carbonate removal to be a very likely reason contributing to the measured $F^{14}C$ DOC-WIOC, i.e. resulting dating offset (Figure 5). Instead of a correction, which does not seem feasible for this effect because of large uncertainties and likely substantial site-to-site (sample-to-sample) variations, we suggest future improvement in the analytical procedure of the carbonate removal step (e.g. a slight increase in acid concentration and an increase of the reaction time).

4.4 $DO^{14}C$ ages in the context of published chronologies

In the following we will discuss our new DO^{14}C results in the context of ages from previous studies. For final calibration of ^{14}C ages, most of those earlier studies took advantage of the assumption of sequential deposition in the archive, i.e. a continuous, undisturbed and preserved sequential deposition of annual snow layers on the glacier surface. Particularly in case of relatively large analytical uncertainties compared to the age difference of the samples, the sequential deposition model can moderately constrain the probability distribution of the calibrated age range in each sample of the dataset. For consistency we applied the same calibration approach here by using the in-built OxCal sequence model (Ramsey, 2008). While the underlying assumption may not generally be valid for all sites, and individually needs to be carefully assessed, we find no difference in the calibrated ages using the sequence model and the ages from the conventional calibration approach for all DO^{14}C data presented in this study (Table 3). Note, that no correction for a potential in-situ ^{14}C bias was applied to the DO^{14}C data used here (Section 4.2).

We obtained the oldest age of ~21 kyr cal BP for the bedrock ice at Belukha, indicating this glacier to be oldest and of Pleistocene origin. This is older than the previously reported age of ~11 kyr cal BP (Table 5, Figure 6). The latter age was obtained for an ice core from the nearby Belukha West Plateau glacier extracted in 2003 (B03) (Aizen et al., 2016; Uglietti et al., 2016) opposed to the 2018 core extracted from the saddle (B18) analyzed in this study. Also, the according sample from B03 was from a slightly shallower depth (0.6-0.3 m above bedrock) than the sample analyzed from B18 in this study. The age range modeled for B03 for the same depth above bedrock (0.5-0 m) is in better agreement with ~28 kyr cal BP and a very large uncertainty of ~15 kyr (Uglietti et al., 2016). Overall, our new age for the oldest ice at Belukha thus reasonably agrees with the previous result but yields a much better constrained age with a reduced uncertainty of ±4 kyr. The two glaciers from the Tibetan Plateau (SLNS and Chongce) show very similar bottom ages of ~5-6 kyr cal BP (Figure 6), which is in agreement with the previously reported age range of Tibetan Plateau glaciers (Hou et al., 2018). The bottom age of Chongce Core 1 determined here based on DO^{14}C (5.6 ± 0.3 kyr cal BP) is slightly younger than the previously reported bottom age in Core 2 based on WIO^{14}C (6.3 ± 0.3 kyr cal BP, Hou et al., 2018), which is in agreement with the findings discussed in Section 4.2 and 4.3. Nevertheless, our new age is still in the range of the previously estimated bottom age (Table 5, Figure 6). The bottom most sample of the Colle Gnifetti 2015 (CG15) core could not be dated because the small amount of ice available yielded an insufficient carbon mass of <10 µg for ^{14}C analysis. Previous WIO^{14}C dating of a core obtained at Colle Gnifetti in 2003

(CG03) also revealed ice of Pleistocene origin with the ice at bedrock being older than 15 kyr cal BP (Jenk et al., 2009). As expected, the age obtained in this study from a shallower depth was much younger with 1.2 kyr cal BP. This is in excellent agreement with the age of CG03 for a similar depth (~74 m below surface; Table 5, Figure 6). We consider this as a clear indication that the CG15 ice core did not reach bedrock.

Overall, the dating with DO^{14}C results in ages which are in good agreement with the age ranges reported in earlier studies. Even though a contribution from in-situ ^{14}C to DO^{14}C was not considered in the comparison here, we find that the dating by the DOC fraction does not lead to significantly different results compared to dating by WIO^{14}C or cause a different interpretation about the oldest ice still present for any of the sites.

5 Conclusion

In this study, we evaluated and successfully validated the DO^{14}C dating technique by direct comparison of dating results with the well-established WIO^{14}C method using parallel ice samples. Achieving this goal was not only analytically demanding but also highly challenging due to the very limited availability of the sampling material, requiring ice in rather large quantities and spanning a wide range of ages. The obtained DO^{14}C ages for four different Eurasian glaciers, ranging from 0.2 ± 0.2 to 20.3 ± 4.1 kyrs cal BP, agreed well with the respective WIO^{14}C ages (0.8 ± 0.4 to 22.4 ± 1.1 kyrs cal BP) and with previously published chronologies from these ice core sites. This underlines the great potential for applying DO^{14}C analysis for ice core dating. With this new method, an average dating uncertainty of around ±200 years was achieved for samples with an absolute carbon mass of > 20 µg and ages up to ~6 kyrs. For DOC concentrations observed in this study, an initial ice mass of about 250 g was required. Our data confirmed previous results that concentrations of pre-industrial DOC are higher by about a factor two compared to WIOC concentrations in high alpine ice cores. This shows that the required ice mass to achieve similar precision is reduced by at least a factor of two for ^{14}C dating when using the DOC instead of the WIOC fraction. Accordingly, an improvement in precision can be achieved for same sample mass. Compared to WIOC, a downside of using the DOC fraction for ^{14}C dating is a more demanding and time consuming extraction procedure. In addition, because of its higher solubility and a related higher mobility of DOC in case of meltwater formation, this fraction is only applicable for dating ice which

had been cold throughout its "lifetime". Beneficial compared to WIOC, there is no potential for a dating bias by carbonates of mineral dust for DO^{14}C. However, our results confirm previously suggested potential dating biases from in-situ ^{14}C causing DO^{14}C dates to shift towards younger ages. While we find the effect to be small (at the level of analytical uncertainty), it may become significant for DO^{14}C dating of ice samples from sites of e.g. exceptional high altitude, experiencing low annual net accumulation rates in addition. For such sites, a reasonably accurate correction to account for the age bias seems feasible according to our results, although at the cost of an increase in the final dating uncertainty. Nevertheless, we think this new dating method has a great potential to open up new fields for radiocarbon dating of ice for example from remote regions, where concentrations of organic impurities in the ice are particularly low.

Acknowledgements

We thank Johannes Schindler for his great work in designing and building the DOC extraction system and the two drilling teams on Colle Gnifetti and Belukha for collecting high quality ice cores. We acknowledge funding from the Swiss National Science Foundation (SNF) for the Sinergia project Paleo fires from high-alpine ice cores (CRSII2_154450), which allowed ice core drilling on Colle Gnifetti and Belukha, for the project Radiocarbon dating of glacier ice (200021_126515), and for the project Reconstruction of pre-industrial to industrial changes of organic aerosols from glacier ice cores (200021_182765). We acknowledge the funding from the National Natural Science Foundation of China (91837102, 41830644) for the Tibetan ice core drilling. We dedicate this study to Alexander Zapf, who died tragically while climbing in the Swiss Alps, before he could fulfil his dream of ice dating with DO^{14}C.

Data availability

The data is provided in the Tables.

Author contributions

LF and TS performed ^{14}C analysis. LF, TS, TMJ, and MS wrote the manuscript while all authors contributed to the discussion of the results. MS designed the study.

Competing interests

The authors declare that they have no conflict of interest.

References

Agrios, K., Salazar, G., Zhang, Y.-L., Uglietti, C., Battaglia, M., Luginbühl, M., Ciobanu, V. G., Vonwiller, M. and Szidat, S.: Online coupling of pure O_2 thermo-optical methods–^{14}C AMS for source apportionment of carbonaceous aerosols, Nucl. Instrum. Methods Phys. Res. B., 361, 288-293, https://doi.org/10.1016/j.nimb.2015.06.008 , 2015.

Agrios, K., Salazar, G. and Szidat, S.: A Continuous-Flow Gas Interface of a Thermal/Optical Analyzer With ^{14}C AMS for Source Apportionment of Atmospheric Aerosols, Radiocarbon, 59, 921-932, https://doi.org/10.1017/RDC.2016.88 , 2017.

Aizen, E. M., Aizen, V. B., Takeuchi, N., Mayewski, P. A., Grigholm, B., Joswiak, D. R., Nikitin, S. A., Fujita, K., Nakawo, M. and Zapf, A.: Abrupt and moderate climate changes in the mid-latitudes of Asia during the Holocene, J. Glaciol., 62, 411-439, https://doi.org/10.1017/jog.2016.34 , 2016.

Bolzan, J. F.: Ice flow at the Dome C ice divide based on a deep temperature profile, J. Geophys. Res. Atmos., 90, 8111-8124, https://doi.org/10.1029/JD090iD05p08111, 1985.

ChongYi, E., Sun, Y., Li, Y. and Ma, X., The atmospheric composition changes above the West Kunlun Mountain, Qinghai-Tibetan Plateau, International Conference on Civil, Transportation and Environment, Atlantis Press, 2016.

Fang, L., Schindler, J., Jenk, T., Uglietti, C., Szidat, S. and Schwikowski, M. J. R.: Extraction of Dissolved Organic Carbon from Glacier Ice for Radiocarbon Analysis, Radiocarbon, 61, 681-694, https://doi.org/10.1017/RDC.2019.36 , 2019.

Fang L., Cao F., Jenk T. M., Vogel A. L., Zhang Y.L., Wacker L., Salazar G., Szidat S., Schwikowski M.: Enhancement of carbonaceous aerosol during the 20th century by anthropogenic activities: insights from an Alpine ice core, in preparation.

Gavin, D. G., Estimation of inbuilt age in radiocarbon ages of soil charcoal for fire history studies. Radiocarbon 43, 27-44, 2001.

Gordon, M. S., Goldhagen, P., Rodbell, K. P., Zabel, T. H., Tang, H. H. K., Clem, J. M., & Bailey, P. Measurement of the flux and energy spectrum of cosmic-ray induced neutrons on the ground. IEEE Transactions on Nuclear Science, 51(6), 3427-3434, 2004.

Hoffmann H. M. Micro radiocarbon dating of the particulate organic carbon fraction in Alpine glacier ice: method refinement, critical evaluation and dating applications, PhD dissertation, Ruperto-Carola University of Heidelberg, http://archiv.ub.uniheidelberg.de/volltextserver/20712/, 2016.

Hoffmann, H., Preunkert, S., Legrand, M., Leinfelder, D., Bohleber, P., Friedrich, R., & Wagenbach, D., A New Sample Preparation System for Micro-14C Dating of Glacier Ice with a First Application to a High Alpine Ice Core from CG (Switzerland). Radiocarbon, 60(2), 517-533. doi:10.1017/RDC.2017.99, 2018.

Hou, S., Jenk, T. M., Zhang, W., Wang, C., Wu, S., Wang, Y., Pang, H. and Schwikowski, M. J. T. C.: Age ranges of the Tibetan ice cores with emphasis on the Chongce ice cores, western Kunlun Mountains, The Cryosphere, 12, 2341-2348, https://doi.org/10.5194/tc-12-2341-2018, 2018.

Hou, S., Zhang W., Fang L., Jenk T.M., Wu S., Pang H., Schwikowski M., Brief Communication: New evidence further constraining Tibetan ice core chronologies to the Holocene, Submitted to The Cryosphere.

Jenk, T. M., Szidat, S., Schwikowski, M., Gaggeler, H. W., Brutsch, S., Wacker, L., Synal, H. A. and Saurer, M.: Radiocarbon analysis in an Alpine ice core: record of anthropogenic and biogenic contributions to carbonaceous aerosols in the past (1650-1940), Atmos. Chem. Phys., 6, 5381-5390, 2006.

Jenk, T. M., Szidat, S., Schwikowski, M., Gäggeler, H., Wacker, L., Synal, H.-A. and Saurer, M.: Microgram level radiocarbon (^{14}C) determination on carbonaceous particles in ice, Nucl. Instrum. Methods Phys. Res. B., 259, 518-525, https://doi.org/10.1016/j.nimb.2007.01.196, 2007.

Jenk, T. M., Szidat, S., Bolius, D., Sigl, M., Gaeggeler, H. W., Wacker, L., Ruff, M., Barbante, C., Boutron, C. F. and Schwikowski, M.: A novel radiocarbon dating technique applied to an ice core from the Alps indicating late Pleistocene ages, J Geophys. Res. Atmos., 114, https://doi.org/10.1029/2009JD011860, 2009.

Lal, D., K. Nishiizumi, and J. R. Arnold.: In situ cosmogenic 3H, 14C, and 10Be for determining the net accumulation and ablation rates of ice sheets, Journal of Geophysical Research: Solid Earth 92.B6 4947-4952, 1987.

Lal, Devendra: Cosmogenic in situ radiocarbon on the earth, Radiocarbon After Four Decades, Springer, New York, NY, 146-161, 1992.

Lal, D., Jull, A. T., Burr, G. and Donahue, D.: Measurements of in situ ^{14}C concentrations in Greenland Ice Sheet Project 2 ice covering a 17 - kyr time span: Implications to ice flow dynamics, J. Geophys. Res. Oceans, 102, 26505-26510, https://doi.org/10.1029/96JC02224, 1997.

Legrand, M., Preunkert, S., Schock, M., Cerqueira, M., Kasper-Giebl, A., Afonso, J., Pio, C., Gelencsér, A. and Dombrowski-Etchevers, I.: Major 20th century changes of carbonaceous aerosol components (EC, WinOC, DOC, HULIS, carboxylic acids, and cellulose) derived from Alpine ice cores, J. Geophys. Res. Atmos., 112, https://doi.org/10.1029/2006JD008080, 2007.

Legrand, M., Preunkert, S., Jourdain, B., Guilhermet, J., Fain, X., Alekhina, I. and Petit, J. R.: Water-soluble organic carbon in snow and ice deposited at Alpine, Greenland, and Antarctic sites: a critical review of available data and their atmospheric relevance, Clim. Past Discuss., 9, 2357-2399, doi:10.5194/cpd-9-2357-2013, 2013.

Licciulli, C., Bohleber, P., Lier, J., Gagliardini, O., Hoelzle, M. and Eisen, O.: A full Stokes ice-flow model to assist the interpretation of millennial-scale ice cores at the high-Alpine drilling site Colle Gnifetti, Swiss/Italian Alps, J. Glaciol., 66, 35-48, https://doi.org/10.1017/jog.2019.82, 2020.

May, B. L. Radiocarbon microanalysis on ice impurities for dating of Alpine glaciers, Ph.D. thesis, University of Heidelberg, Germany, 127pp., 2009.

May, B., Wagenbach, D., Hoffmann, H., Legrand, M., Preunkert, S. and Steier, P.: Constraints on the major sources of dissolved organic carbon in Alpine ice cores from radiocarbon analysis over the bomb - peak period, J. Geophys. Res. Atmos., 118, 3319-3327, https://doi.org/10.1002/jgrd.50200, 2013.

Masarik, J., and Reedy, R. C. : Terrestrial cosmogenic-nuclide production systematics calculated. Earth and Planet. Sci. Lett. 136, 381-395, 1995.

Minguillon MC, Perron N, Querol X, Szidat S, Fahrni SM, Alastuey A, et al. Fossil versus contemporary sources of fine elemental and organic carbonaceous particulate matter during the DAURE campaign in Northeast Spain, Atmos. Chem. Phys. 11, 12067-12084, 2011.

584 Mohn, J., Szidat, S., Fellner, J., Rechberger, H., Quartier, R., Buchmann, B., & Emmenegger, L.
585 Determination of biogenic and fossil CO_2 emitted by waste incineration based on $^{14}CO_2$ and mass
586 balances. Bioresource Technology 99, 6471-6479, 2008.

587 Nye, J.: On the theory of the advance and retreat of glaciers, Geophys. J. Int., 7, 431-456, 1963.

588 Petrenko, V. V., Severinghaus, J. P., Smith, A. M., Riedel, K., Baggenstos, D., Harth, C., Orsi, A., Hua,
589 Q., Franz, P., Takeshita, Y., Brailsford, G., Weiss, R. F., Buizert, C., Dickson, A., Schaefer, H.: High-
590 precision ^{14}C measurements demonstrate production of insitu cosmogenic $^{14}CH_4$ and rapid loss of
591 insitu cosmogenic ^{14}CO in shallow Greenland firn. Earth and Planet. Sci. Lett. 365,190–197,2013.

592 Ramsey, C. B.: Deposition models for chronological records, Quat. Sci. Rev., 27, 42-60,
593 https://doi.org/10.1016/j.quascirev.2007.01.019, 2008.

594 Ramsey, C. B.: Methods for summarizing radiocarbon datasets, Radiocarbon, 59, 1809-1833,
595 https://doi.org/10.1017/RDC.2017.108, 2017.

596 Reimer, P. J., Bard, E., Bayliss, A., Beck, J. W., Blackwell, P. G., Ramsey, C. B., Buck, C. E., Cheng, H.,
597 Edwards, R. L., Friedrich, M., Grootes, P., Guilderson, T., Haflidason, H., Hajdas, I., Hatté, C., Heaton,
598 T., Hoffmann, D. L., Hogg, A. G., Hughen, K. A., Felix Kaiser, K., Kromer, B., Manning, S. W., Niu, M.,
599 Reimer, R. W., Richards, D. A., Scott, E. M., Southon, J. R., Staff, R. A., Turney, C. S. and van der Plicht,
600 J.: IntCal13 and Marine13 radiocarbon age calibration curves 0–50,000 years cal BP, Radiocarbon, 55,
601 1869-1887, https://doi.org/10.2458/azu_js_rc.55.16947, 2013.

602 Ruff, M., Wacker, L., Gäggeler, H., Suter, M., Synal, H.-A. and Szidat, S.: A gas ion source for
603 radiocarbon measurements at 200 kV, Radiocarbon 49, 307-314,
604 https://doi.org/10.1017/S0033822200042235, 2007.

605 Sigl, M., Jenk, T. M., Kellerhals, T., Szidat, S., Gäggeler, H. W., Wacker, L., Synal, H.-A., Boutron, C.,
606 Barbante, C. and Gabrieli, J.: Towards radiocarbon dating of ice cores, J. Glaciol., 55, 985-996,
607 https://doi.org/10.3189/002214309790794922, 2009.

608 Sigl, M., Abram, N., Gabrieli, J., Jenk, T. M., Osmont, D., and Schwikowski, M., 19th century glacier
609 retreat in the Alps preceded the emergence of industrial black carbon deposition on high-alpine
610 glaciers, The Cryosphere,12,3311-3331, https://doi.org/10.5194/tc-12-3311-2018, 2018.

611 Smith, A., Levchenko, V., Etheridge, D., Lowe, D., Hua, Q., Trudinger, C., Zoppi, U. and Elcheikh, A.: In
612 search of in-situ radiocarbon in Law Dome ice and firn, Nucl. Instrum. Methods Phys. Res. B., 172,
613 610-622, https://doi.org/10.1016/S0168-583X(00)00280-9, 2000.

614 Steier, P., Fasching, C., Mair, K., Liebl, J., Battin, T., Priller, A. and Golser, R., A new UV oxidation
615 setup for small radiocarbon samples in solution. Radiocarbon, 55, 373-382, DOI:
616 10.2458/azu_js_rc.55.16368, 2013.

617 Stuiver, M. and Polach, H. A.: Discussion reporting of ^{14}C data, Radiocarbon 19, 355-363, 1977.

618 Synal, H.-A., Stocker, M. and Suter, M.: MICADAS: a new compact radiocarbon AMS system, Nucl.
619 Instrum. Methods Phys. Res. B., 259, 7-13, https://doi.org/10.1016/j.nimb.2007.01.138, 2007.

620 Szidat, S., Salazar, G. A., Vogel, E., Battaglia, M., Wacker, L., Synal, H.-A. and Türler, A.: ^{14}C analysis
621 and sample preparation at the new Bern Laboratory for the Analysis of Radiocarbon with AMS
622 (LARA), Radiocarbon, 56, 561-566, 10.2458/56.17457,2014.

623 Thompson, L. G., Tandong, Y., Davis, M. E., Mosley-Thompson, E., Mashiotta, T. A., Lin, P.-N.,
624 Mikhalenko, V. N. and Zagorodnov, V. S. J. A. o. G.: Holocene climate variability archived in the

Puruogangri ice cap on the central Tibetan Plateau, Ann. Glaciol., 43, 61-69, https://doi.org/10.3189/172756406781812357, 2006.

Uglietti, C., Zapf, A., Jenk, T. M., Sigl, M., Szidat, S., Salazar Quintero, G. A. and Schwikowski, M.: Radiocarbon dating of glacier ice: overview, optimisation, validation and potential, The Cryosphere 10, 3091-3105, 10.5194/tc-10-3091-2016, 2016.

Van de Wal, R., Van Roijen, J., Raynaud, D., Van der Borg, K., De Jong, A., Oerlemans, J., Lipenkov, V. and Huybrechts, P.: From $^{14}C/^{12}C$ measurements towards radiocarbon dating of ice. Tellus B Chem. Phys. Meteorol., 46, 91-102, https://doi.org/10.3402/tellusb.v46i2.15755, 1994.

Wacker, L., Fahrni, S. M., Hajdas, I., Molnar, M., Synal, H. A., Szidat, S. and Zhang, Y. L.: A versatile gas interface for routine radiocarbon analysis with a gas ion source, Nucl. Instrum. Methods Phys. Res. B., 294, 315-319, https://doi.org/10.1016/j.nimb.2012.02.009, 2013.

Woon, D. E.: Modeling gas-grain chemistry with quantum chemical cluster calculations. I. Heterogeneous hydrogenation of CO and H_2CO on icy grain mantles. The Astrophys. J., 569, 541-548, 2002.

Yankwich, P. E., Rollefson, G. K., and Norris, T. H. (1946). Chemical Forms Assumed by C^{14} Produced by Neutron Irradiation of Nitrogenous Substances. J. Chem. Phys., 14, 131-140,1946.

Zhang, Y. L., Perron, N., Ciobanu, V. G., Zotter, P., Minguillón, M. C., Wacker, L., Prévôt, A. S. H., Baltensperger, U. and Szidat, S.: On the isolation of OC and EC and the optimal strategy of radiocarbon-based source apportionment of carbonaceous aerosols, Atmos. Chem. Phys., 12, 10841-10856, https://doi.org/10.5194/acp-12-10841-2012, 2012.

Zhang, Y., Y. Yao, X. Wang, Y. Liu, andS. Piao, Mapping spatialdistribution of forest age in China,Earth and Space Science,4, 108–116,doi:10.1002/2016EA000177, 2017.

Table 1 WIOC samples analyzed from Colle Gnifetti, Belukha, SLNS and Chongce ice cores.

Core section	Depth (m)	Ice mass (kg)	WIOC (µg)	Concentration (µg/kg)	Bern AMS Nr.	$F^{14}C$ (±1σ)	^{14}C age (BP, ±1σ)
CG110	72.1-72.7	0.570	35.2	61.9±3.3	11770.1.1	0.875±0.011	1073±105
CG111	72.7-73.4	0.539	38.7	71.8±3.8	11771.1.1	0.848±0.011	1321±101
CG112	73.4-73.9	0.536	23.7	44.1±2.4	11772.1.1	0.852±0.015	1284±143
CG113	73.9-74.6	0.549	39.8	72.4±3.8	11773.1.1	0.786±0.011	1937±109
Belukha412	158.3-159.0	0.443	37.8	85.2±4.5	11766.1.1	0.367±0.010	8055±211
Belukha414	159.5-160.3	0.336	27.8	82.6±4.4	11768.1.1	0.212±0.014	12473±535
Belukha415	160.3-160.9	0.319	39.3	123.3±6.5	11769.1.1	0.100±0.011	18462±899
SLNS101	56.8-57.5	0.420	41.5	98.9±2.1	12325.1.1	0.902±0.047	825±420
SLNS113	64.7-65.4	0.427	45.3	106.1±2.5	12324.1.1	0.852±0.046	1284±438
SLNS122	68.9-69.7	0.424	58.5	138.0±3.6	12323.1.1	0.807±0.046	1727±459
SLNS127	71.8-72.5	0.483	50.9	105.3±2.5	12322.1.1	0.695±0.046	2921±532
SLNS136	76.7-77.5	0.374	50.6	135.2±3.0	12321.1.1	0.521±0.046	5235±706
SLNS139	78.9-79.6	0.485	61.2	126.3±3.6	12320.1.1	0.521±0.045	5232±703
SLNS141-142	80.3-81.0	0.413	61.7	149.5±3.8	12319.1.1	0.489±0.046	5754±750
CC237	126.0-126.7	0.352	22.4	63.7±1.8	12328.1.1	0.704±0.049	2815±555
CC244	130.2-130.8	0.311	29.8	95.9±2.2	12327.1.1	0.639±0.048	3602±600
CC252	133.4-133.8	0.174	23.8	136.7±4.3	12326.1.1	0.316±0.049	9256±1250

Table 2 DOC samples analyzed for Colle Gnifetti, Belukha, SLNS and Chongce ice cores.

Core section	Depth (m)	Ice mass (kg)	DOC (µg)	Concentration (µg/kg)	Bern AMS Nr.	$F^{14}C$ (±1σ)	^{14}C age (BP, ±1σ)	DOC/WIOC
CG110	72.1-72.7	0.171	18.9	110.0±2.7	11575.1.1	0.943±0.030	474±259	1.8
CG111	72.7-73.4	0.207	25.5	122.9±3.0	11576.1.1	0.901±0.021	836±190	1.7
CG112	73.4-73.9	0.248	23.6	95.0±2.3	11577.1.1	0.889±0.021	943±192	2.2
CG113	73.9-74.6	0.246	29.5	119.4±2.9	11578.1.1	0.849±0.016	1312±151	1.7
Belukha412	158.3-159.0	0.172	28.5	165.0±4.0	11581.1.1	0.315±0.024	9284±624	1.9
Belukha414	159.5-160.3	0.128	41.9	327.4±7.9	11584.1.1	0.239±0.019	11505±648	4.0
Belukha415	160.3-160.9	0.102	23.7	231.0±5.6	11585.1.1	0.144±0.041	15584±2365	1.9
SLNS101	56.8-57.5	0.238	44.0	184.9±4.5	12458.1.1	0.972±0.016	227±131	1.9
SLNS113	64.7-65.4	0.213	39.4	185.2±4.5	12459.1.1	0.942±0.016	484±137	1.7
SLNS122	68.9-69.7	0.234	57.9	248.0±6.0	12460.1.1	0.773±0.010	2073±101	1.8
SLNS127	71.8-72.5	0.252	57.8	229.7±5.5	12461.1.1	0.730±0.009	2527±101	2.2
SLNS136	76.7-77.5	0.220	48.3	219.1±5.3	12462.1.1	0.657±0.009	3380±112	1.6
SLNS139	78.9-79.6	0.208	48.1	230.8±5.6	12463.1.1	0.580±0.009	4381±131	1.8
SLNS141-142	80.3-81.0	0.246	43.8	177.5±4.3	12464.1.1	0.550±0.010	4809±151	1.2
CC237	126.0-126.7	0.208	28.5	136.6±3.3	12454.1.1	0.980±0.023	161±185	2.1
CC244	130.2-130.8	0.167	21.7	129.8±3.1	12455.1.1	0.800±0.018	1789±185	1.4
CC252	133.4-133.8	0.120	24.3	202.5±4.9	12456.1.1	0.546±0.016	4854±239	1.5

Table 3 Calibrated WIO^{14}C and DO^{14}C ages using OxCal v4.3.2 with the Intcal13 radiocarbon calibration curve. Ages are given as the OxCal provided μ-age ± 1σ, which is the calibrated mean age accounting for the age probability distribution. In addition, calibrated ages derived when applying the OxCal sequence deposition model for further constraint are shown.

Core section	WIOC Cal age (cal BP)	WIOC Cal age with sequence (cal BP)	DOC Cal age (cal BP)	DOC Cal age with sequence (cal BP)
CG110	1004±119	968±1049	464±235	403±196
CG111	1224±103	1174±86	810±169	749±123
CG112	1190±142	1292±103	901±176	947±139
CG113	1889±138	1869±143	1222±153	1248±144
Belukha412	8960±266	8954±268	10695±867	10686±865
Belukha414	14796±782	14802±774	13646±893	13670±880
Belukha415	22441±1107	22497±1107	20264±4073	20393±4033
SLNS101	848±396	701±315	250±145	226±137
SLNS113	1297±453	1255±331	480±131	505±111
SLNS122	1769±514	1901±4301	2057±129	2056±129
SLNS127	3175±679	3221±629	2585±125	2585±125
SLNS136	6030±824	5426±620	3635±138	3636±137
SLNS139	6026±820	6177±567	5014±191	5007±187
SLNS141-142	6626±831	7081±689	5519±188	5531±176
CC237	3051±703	2886±617	237±151	233±153
CC244	4057±769	4210±713	1737±211	1738±212
CC252	11000±1697	11017±1716	5580±294	5580±295

Table 4 Estimate of the effect from in-situ ^{14}C production on $F^{14}C$-DOC. For comparison, the measured $F^{14}C$ offset between DOC and WIOC is also shown.

Core section	Ice mass (g)	Carbon mass (µg)	Depth (m w.e.)	P_o (^{14}C atom g^{-1} ice yr^{-1})	In-situ ^{14}C (atoms)	In-situ $F^{14}C$-DOC offset	Observed $F^{14}C$ DOC-WIOC offset	In-situ corrected $F^{14}C$-DOC	In-situ corrected DOC Cal age (cal BP)
CG110	171	18.9	55.8	328	1197	0.033±0.013	0.068±0.032	0.910±0.033	752±273
CG111	207	25.5	56.3	328	1197	0.030±0.012	0.053±0.024	0.901±0.024	1045±207
CG112	248	23.6	56.7	328	1197	0.038±0.015	0.037±0.026	0.889±0.026	1225±250
CG113	246	29.5	57.0	328	1197	0.030±0.012	0.064±0.019	0.849±0.020	1546±208
Belukha412	172	28.5	142.7	286	921	0.017±0.007	-0.052±0.026	0.315±0.025	11271±902
Belukha414	128	41.9	143.9	286	921	0.009±0.003	0.027±0.024	0.239±0.020	14096±964
Belukha415	102	23.7	144.5	286	921	0.012±0.005	0.043±0.043	0.144±0.041	21571±4753
SLNS101	238	44	47.9	345	2666	0.044±0.017	0.070±0.050	0.972±0.023	587±187
SLNS113	213	39.4	54.4	345	2656	0.044±0.017	0.089±0.050	0.942±0.023	837±184
SLNS122	234	57.9	58.1	345	2651	0.033±0.013	-0.034±0.047	0.773±0.016	2483±210
SLNS127	183	57.8	60.5	345	2647	0.026±0.010	0.029±0.047	0.730±0.014	2967±197
SLNS136	220	48.3	64.7	345	2641	0.037±0.014	0.135±0.047	0.657±0.017	4264±304
SLNS139	208	48.1	66.5	345	2638	0.035±0.014	0.058±0.046	0.580±0.016	5600±290
SLNS141-142	246	43.8	67.7	345	2636	0.045±0.018	0.061±0.047	0.550±0.020	6323±363
CC237	208	28.5	113.7	497	5371	0.120±0.046	0.275±0.054	0.980±0.052	1240±498
CC244	167	21.7	117.6	497	5353	0.126±0.049	0.161±0.051	0.800±0.052	3509±799
CC252	120	24.3	120.2	497	5341	0.080±0.031	0.231±0.051	0.546±0.035	7007±635

Table 5 DO^{14}C dating results for near bedrock ice compared to results from previous studies (visualized in Figure 6).

Site	Study	Core	Dating method	Depth above bedrock (m)	Age (cal BP)
Colle Gnifetti	this study	CG15	DO^{14}C	(74.3 m below surface)*	1248 ± 144
	Jenk et al., 2009	CG03	WIO^{14}C	(73.5 m below surface)#	1152 ± 235
	Jenk et al., 2009	CG03	Model	(74.3 m below surface)&	$1160 \pm^{140}_{170}$
	Jenk et al., 2009	CG03	WIO^{14}C	0.6-0	>15000
	Jenk et al., 2009	CG03	Model	oldest ice estimate	$19100 \pm^{4800}_{4500}$
Belukha	this study	B18 (saddle)	DO^{14}C	0.5-0	20393 ± 4033
	Aizen et al., 2016	B03 (west plateau)	WIO^{14}C	0.6-0.3	11015 ± 1221
	Uglietti et al., 2016	B03 (west plateau)	Model	0.6-0	28500 ± 16200
SLNS	this study	SLNS	DO^{14}C	0.4-0	5531 ± 176
	no previous results		---	---	---
Chongce	this study	Core 1	DO^{14}C	0.2-0	5580 ± 295
	Hou et al., 2018	Core 2	WIO^{14}C	1.2-0.8	6253 ± 277
	Hou et al., 2018	Core 2	Model	oldest ice estimate	$9000 \pm^{7900}_{3600}$

*precise bedrock depth unknown at this coring site, #sampled depth being closest to depth sampled in this study (CG03 and CG15 drill sites only 16 m apart), &modeled age at same depth as sampled in this study.

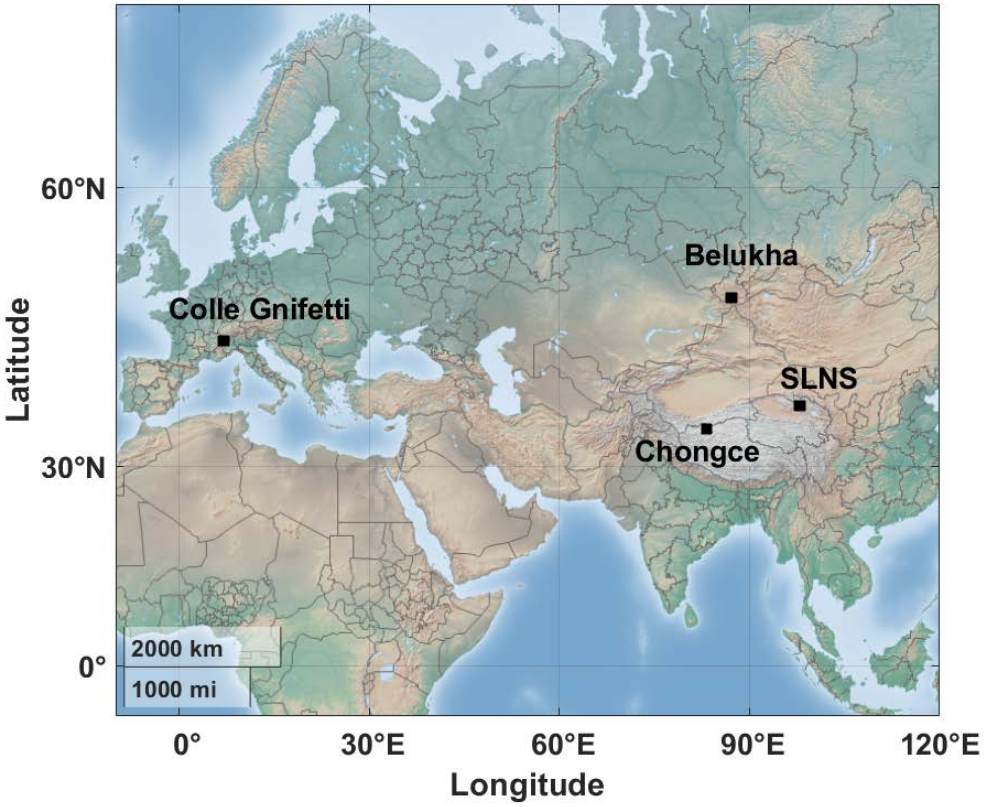

Figure 1: Location of the four glaciers Colle Gnifetti, Belukha, Chongce, and Shu Le Nan Shan (SLNS). Map made from Matlab R2019b geobasemap. Colle Gnifetti is located in the Monte Rosa massif in the Swiss Alps, Belukha glacier in the Altai mountain range, Russia, the Chongce ice cap on the northwestern Tibetan Plateau, China, and the SLNS at the south slope of the Shulenanshan Mountain, China.

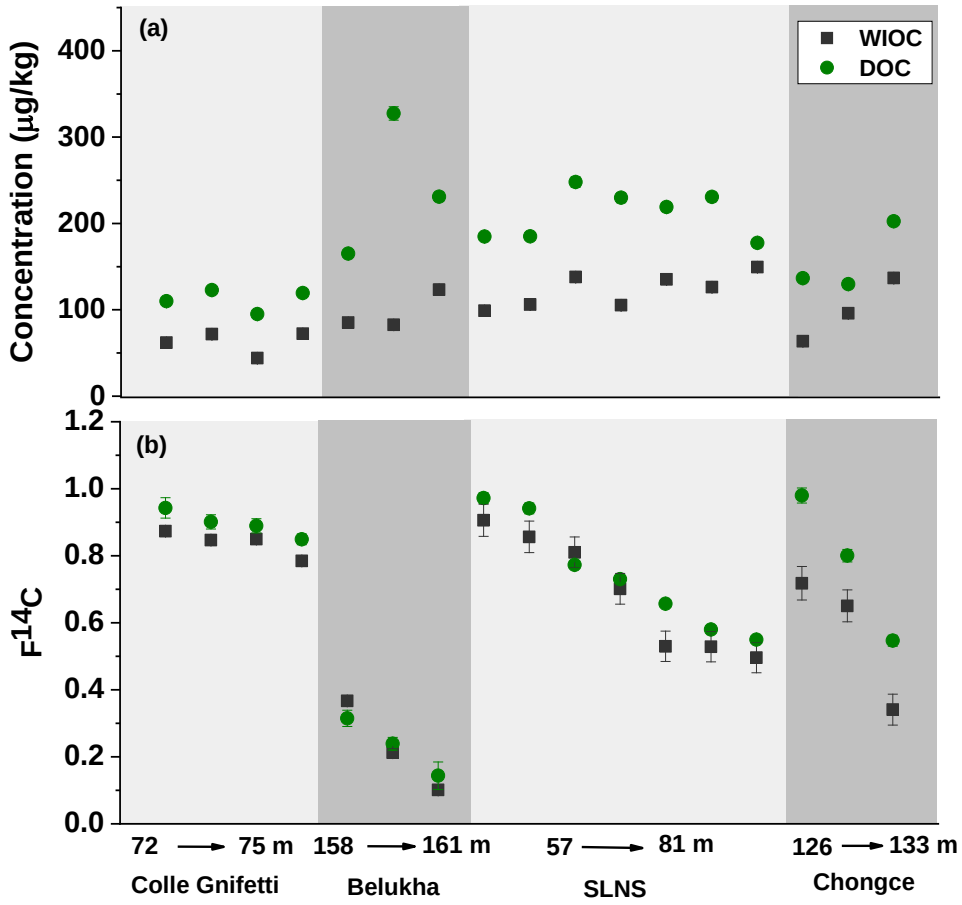

Figure 2: Comparison of results from the WIOC and DOC fractions for the studied four sites. (a) concentrations (b) $F^{14}C$. The error bars denote the overall analytical 1σ uncertainty.

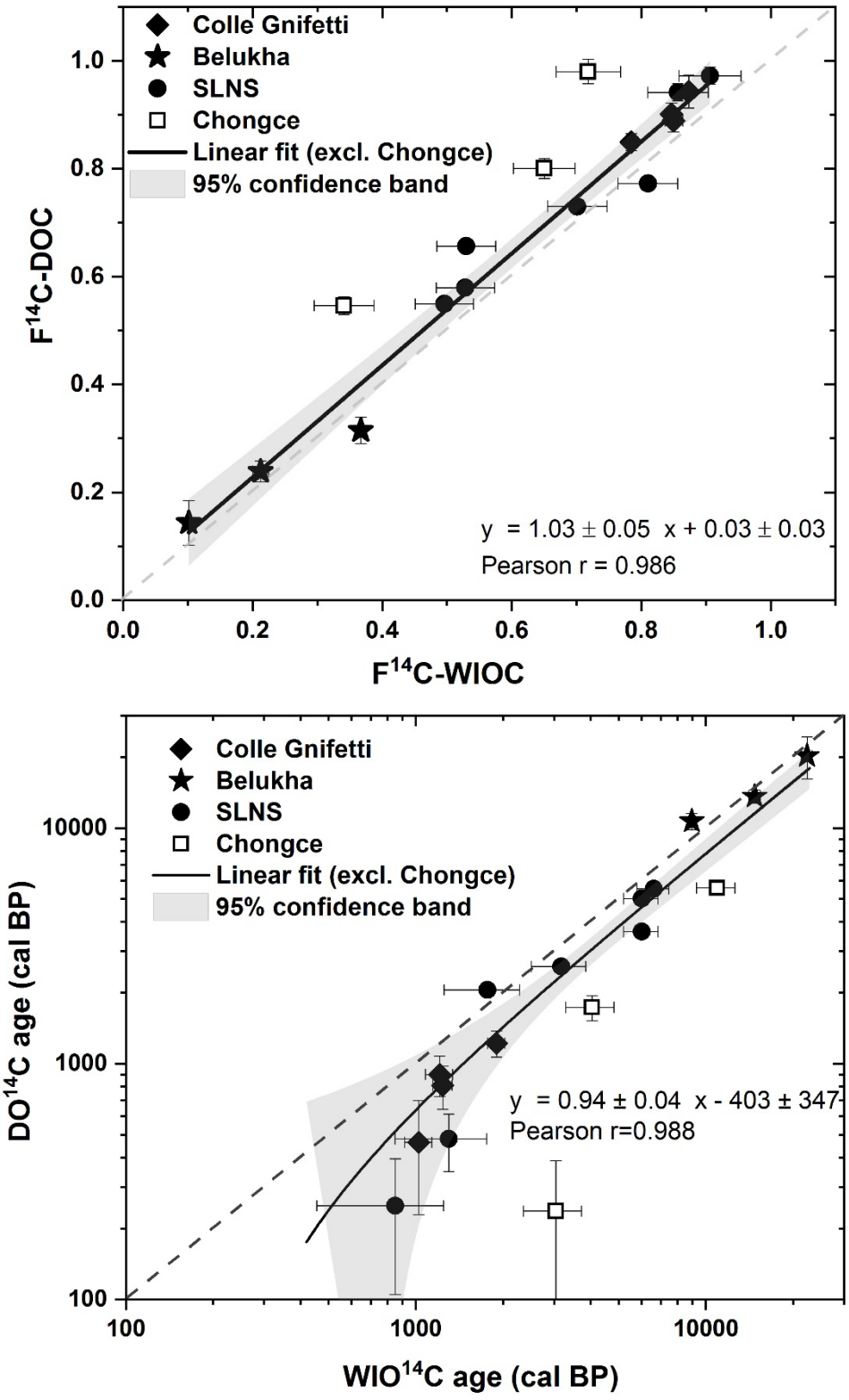

Figure 3 Scatter plot showing the correlation between WIO^{14}C and DO^{14}C results for the four sites (see legend). In terms of F^{14}C (top) and calibrated ages (bottom). For the linear fit in both panels, the data from Chongce (open symbols) was excluded. Shaded areas indicate the 95% confidence band.

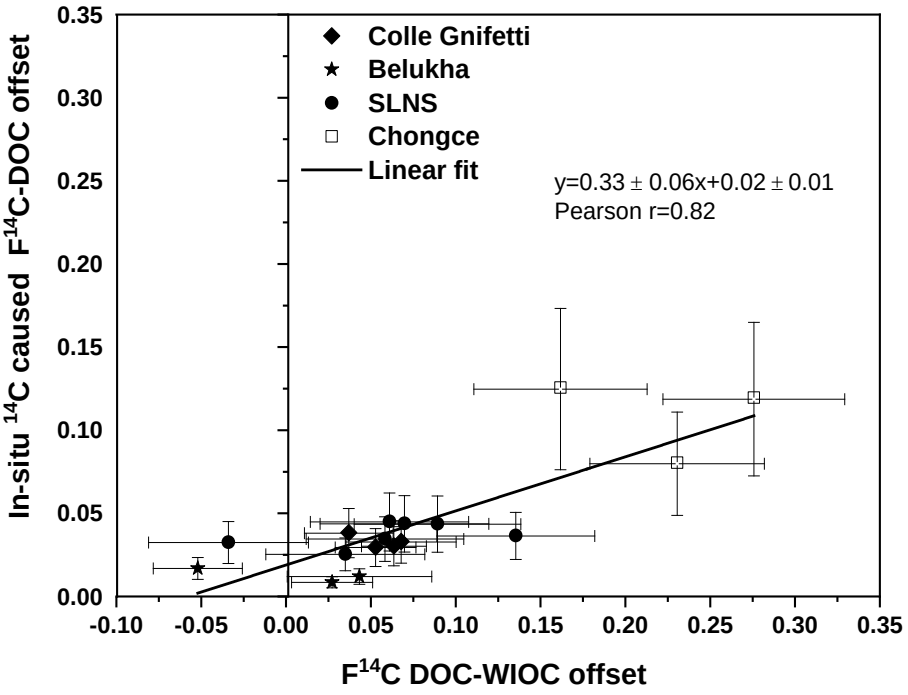

Figure 4 Estimated in-situ ^{14}C offset to $F^{14}C$-DOC plotted against the measured offset between $F^{14}C$ of the DOC and WIOC fraction.

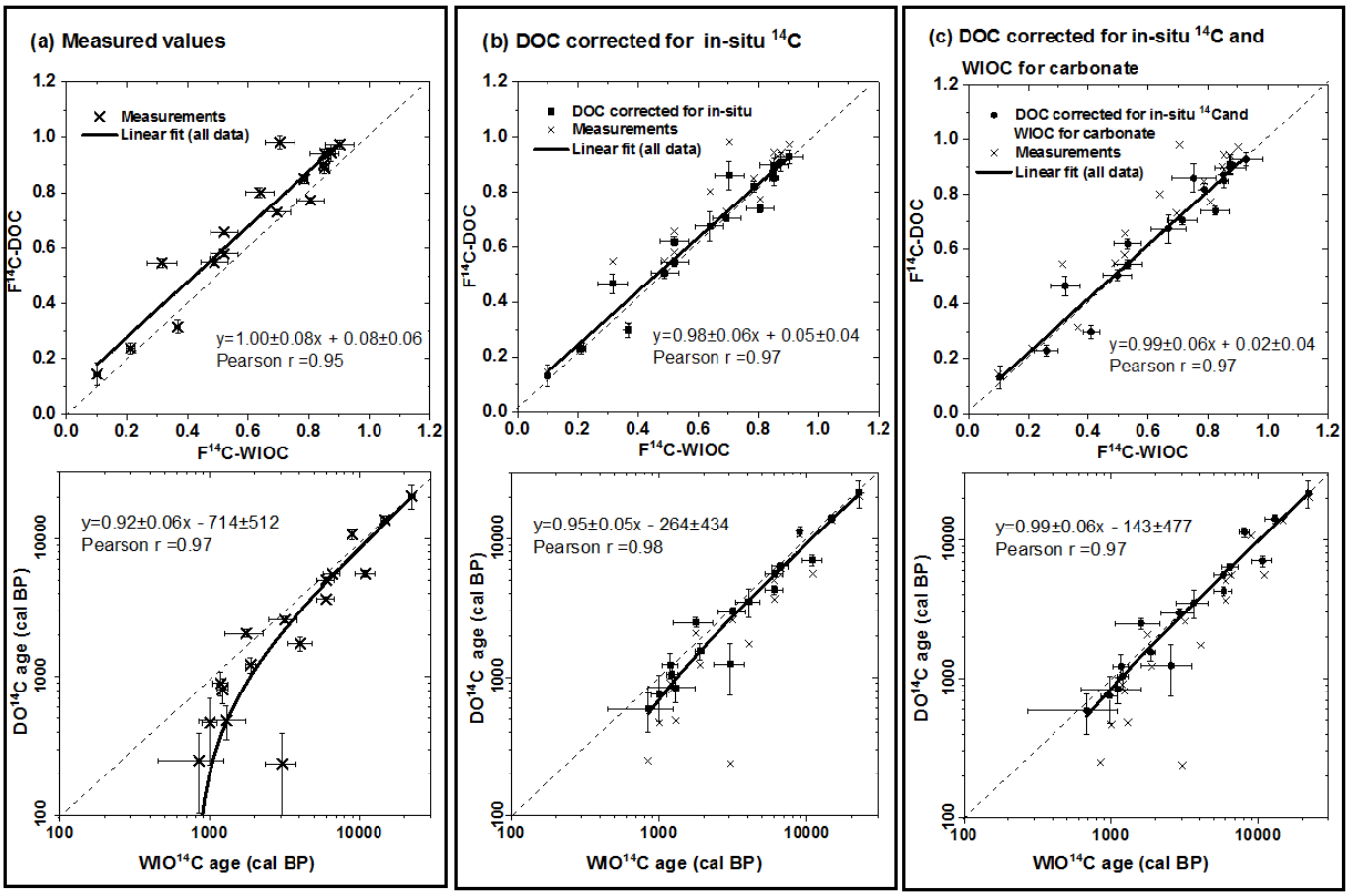

Figure 5 Scatter plots showing the correlation between WIO^{14}C and DO^{14}C results for all samples. In terms of F^{14}C (top) and calibrated ages (bottom). (a) Measured values as shown in Figure 3 but with the linear fit applied to all data (Chongce included). (b) Same as panel (a), but DOC ^{14}C results corrected for in-situ ^{14}C contribution. (c) Same as panel (a), but DOC and WIOC ^{14}C results corrected for in-situ ^{14}C and accounting for potentially incompletely removed carbonate, respectively. An estimated average carbonate removal efficiency of 98±2 % was used here. Error bars in panel (a) and (b) reflect the propagated uncertainty of analysis and correction. In panel (b) and (c), measured values are shown as gray crosses.

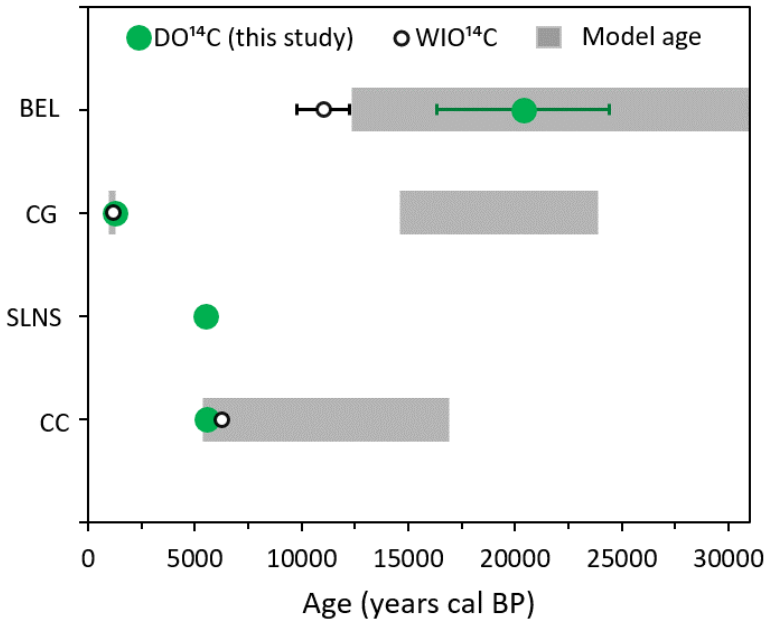

Figure 6 Comparison of our DO^{14}C ages (not corrected for in-situ) with dating results from previous studies if available. For the four sites of Belukha (BEL), Colle Gnifetti (CG), Shu Le Nan Shan (SLNS) and Chongce (CC), DO^{14}C ages (green) and previously reported WIO^{14}C ages (open circles) for similar sampling depths are shown. Gray bars indicate previously modeled, ^{14}C based bedrock age estimates (additionally for CG the modeled age for the bottom sampling depth of this study). Previously published data are from Uglietti et al. (2016) (BEL, West Plateau), Jenk et al. (2009) (CG), and Hou et al. (2018) (CC). See Table 5 for underlying data and details.